

# UC Irvine

## UC Irvine Previously Published Works

### Title

Mechanism of water extraction from gypsum rock by desert colonizing microorganisms

### Permalink

<https://escholarship.org/uc/item/01n9g84v>

### Journal

Proceedings of the National Academy of Sciences of the United States of America, 117(20)

### ISSN

0027-8424

### Authors

Huang, Wei  
Ertekin, Emine  
Wang, Taifeng  
[et al.](#)

### Publication Date

2020-05-19

### DOI

10.1073/pnas.2001613117



### Copyright Information

This work is made available under the terms of a Creative Commons Attribution-NonCommercial-NoDerivatives License, available at <https://creativecommons.org/licenses/by-nc-nd/4.0/>

Peer reviewed



# Mechanism of water extraction from gypsum rock by desert colonizing microorganisms

Wei Huang<sup>a</sup>, Emine Ertekin<sup>b</sup>, Taifeng Wang<sup>c</sup>, Luz Cruz<sup>c</sup>, Micah Dailey<sup>b</sup>, Jocelyne DiRuggiero<sup>b</sup> , and David Kisailus<sup>a,c,d,1</sup> 

<sup>a</sup>Department of Chemical and Environmental Engineering, University of California, Riverside, CA 92521; <sup>b</sup>Department of Biology, Johns Hopkins University, Baltimore, MD 21218; <sup>c</sup>Materials Science and Engineering Program, University of California, Riverside, CA 92521; and <sup>d</sup>Department of Materials Science and Engineering, University of California, Irvine, CA 92697

Edited by Donald E. Canfield, Institute of Biology and Nordic Center for Earth Evolution, University of Southern Denmark, Odense M., Denmark, and approved March 30, 2020 (received for review January 28, 2020)

**Microorganisms, in the most hyperarid deserts around the world, inhabit the inside of rocks as a survival strategy. Water is essential for life, and the ability of a rock substrate to retain water is essential for its habitability. Here we report the mechanism by which gypsum rocks from the Atacama Desert, Chile, provide water for its colonizing microorganisms. We show that the microorganisms can extract water of crystallization (i.e., structurally ordered) from the rock, inducing a phase transformation from gypsum ( $\text{CaSO}_4 \cdot 2\text{H}_2\text{O}$ ) to anhydrite ( $\text{CaSO}_4$ ). To investigate and validate the water extraction and phase transformation mechanisms found in the natural geological environment, we cultivated a cyanobacterium isolate on gypsum rock samples under controlled conditions. We found that the cyanobacteria attached onto high surface energy crystal planes ( $\{011\}$ ) of gypsum samples generate a thin biofilm that induced mineral dissolution accompanied by water extraction. This process led to a phase transformation to an anhydrous calcium sulfate, anhydrite, which was formed via reprecipitation and subsequent attachment and alignment of nanocrystals. Results in this work not only shed light on how microorganisms can obtain water under severe xeric conditions but also provide insights into potential life in even more extreme environments, such as Mars, as well as offering strategies for advanced water storage methods.**

microorganisms | water extraction | anhydrite | gypsum | phase transformation

**W**ater plays many roles in organismal function: It is not only critical for metabolic processes but also acts as a structural component in materials and tissues (1, 2). Against all odds, even in the driest places on Earth where nothing grows, microorganisms were found to colonize lithic (rock) substrates as a last refuge for life (3, 4). By filtering out UV irradiation and enhancing access to water, the rock provides protection and stability to an unexpected diversity of microbial taxa, including cyanobacteria, actinobacteria, *Chloroflexus*, and proteobacteria (4, 5). Such assemblies of endolithic (within rock) microorganisms have been found in the Atacama Desert in Chile, one of the driest and oldest deserts on Earth (6–8) and an analogous environment to Mars (9). The aridity index (AI) of the Atacama Desert, the ratio of the average water supply and potential evapotranspiration, can be as low as 0.0075 (10), whereas an AI threshold of 0.05 is used to defined hyperarid deserts (11). In the hyperarid core of the desert, records of air relative humidity (RH) show extensive periods below 60% RH (*SI Appendix, Fig. S1*), illustrating the scarcity of water. It is important to note that 0.585 water activity ( $a_w$ ; 58.5% RH) is the lower limit at which metabolic activity was detected (12). Thus, understanding how microorganisms acquire water under extreme xeric stress could provide insights into potential life on past, or present, Mars, and also help in the development of new technologies for water storage and acquisition (13, 14). Xeric stress is defined here as a lack of water (desiccation) that produces biochemical, metabolic, physical, and physiological stress (1). The range of water activity

for the onset of xeric stress varies from 0.91 $a_w$  to 0.585 $a_w$ , depending the microorganisms (1, 12).

One type of mineral commonly found in the Atacama Desert is gypsum (7), a hydrated calcium sulfate ( $\text{CaSO}_4 \cdot 2\text{H}_2\text{O}$ ). While this substrate contains other minerals, such as sepiolite, that can potentially alleviate xeric stresses due to its porous structure and water absorption and retention abilities (8, 15), the water found within the gypsum is crystalline, with up to 20.8% of the total mass stored within its lattice. Thus, it is reasonable to surmise that gypsum can act as a source of water for organisms living under extreme xeric stress (16). In fact, it was determined that a shallow-rooted plant, *Helianthemum squamatum*, lives on gypsum and extracts water from the rock during dry summers in northeastern Spain (17). However, the mechanism by which this water is exacted from gypsum as well as its resulting effect on the rock remains unidentified.

The transitions between the various phases of geologic calcium sulfate minerals—gypsum, bassanite, and anhydrite—has been studied (15, 18–20). It is known that gypsum may lose some or all of its structural or “crystalline” water and subsequently transforms to either a hemihydrate phase, bassanite ( $\text{CaSO}_4 \cdot 1/2\text{H}_2\text{O}$ ), or an anhydrous phase, anhydrite ( $\text{CaSO}_4$ ), in different environments (18, 22). In addition, gypsum, which has been found in evaporitic minerals in the upper crust of Earth, can undergo a reversible transformation to anhydrite after dehydration–hydration cycling under certain geochemical conditions (18). Phase diagrams of  $\text{CaSO}_4$  and water have been developed to show effects of temperature and pressure on the solubility and stability of different phases (15, 19). Gypsum is the thermodynamically stable phase

## Significance

**This research provides an in-depth analysis of how microorganisms are able to survive in the world’s driest non-polar place, the Atacama Desert, Chile. We show that these organisms extract water from gypsum rocks in this desert, enabling these colonizing microorganisms to sustain life in this extreme environment. We believe the results in this work could not only shed light on how microorganisms can obtain water under severe xeric conditions, but also provide insights into potential life in even more extreme environments, such as Mars, as well as offer strategies for advanced water storage methods.**

Author contributions: W.H., J.D., and D.K. designed research; W.H., E.E., T.W., L.C., and M.D. performed research; W.H., E.E., J.D., and D.K. analyzed data; and W.H., E.E., J.D., and D.K. wrote the paper.

The authors declare no competing interest.

This article is a PNAS Direct Submission.

Published under the [PNAS license](#).

<sup>1</sup>To whom correspondence may be addressed. Email: david.k@uci.edu.

This article contains supporting information online at <https://www.pnas.org/lookup/suppl/doi:10.1073/pnas.2001613117/-DCSupplemental>.

First published May 4, 2020.

below 40 °C, but is unstable with increasing temperature, transforming to the anhydrite phase (19). The kinetics of these gypsum–anhydrite phase transformations are controlled by additional environmental conditions such as acidity and ionic strength, which could potentially affect the hydrogen bonds between water molecules and sulfate ions inside gypsum crystals. For example, the presence of H<sup>+</sup> can facilitate the extraction of water of crystallization (i.e., structurally ordered) inside the gypsum crystals by forming H<sub>3</sub>O<sup>+</sup>, which increases the mineral solubility (20).

Here, we use a combination of microscopy and spectroscopy to characterize gypsum samples from both geological and laboratory environments, revealing the processes by which colonizing microorganisms obtain water from their substrate, and the resulting effect on the rock. We report that gypsum rocks transform to anhydrites because of the loss of water of crystallization in a process induced by microorganisms. The findings in this study will provide insight toward mechanisms of survival for organisms living in extreme environments and thus have potential for use in identifying water storage sources for extraterrestrial exploration or habitation.

### Microorganisms Living in the Gypsum Rocks

Observation of gypsum rock collected in the Atacama Desert showed a green colonization zone under the surface (white arrow in Fig. 1A), indicating the presence of photosynthetic microorganisms (7). Microcomputed tomography (μ-CT) images (Fig. 1B) uncovered microbial colonies inside the rock. In addition, the CT scans revealed the pores present within the rock matrix, and the microorganisms colonizing them, as previously reported (6–8). Further observations provided by scanning electron microscopy (SEM) (Fig. 1C and D) showed that the microorganisms had a preferable attachment to specific crystal facets of gypsum. Raman spectroscopy and mapping (SI Appendix, Fig. S2) and SEM micrographs (SI Appendix, Fig. S3) confirmed that the microbial cells assembled primarily on the {011} planes of gypsum. It is likely that these specific planes have a rougher surface (23), which enables stronger adhesion, but may also facilitate accelerated water access (i.e., via enhanced dissolution kinetics) (24, 25). Cyanobacteria-like cells were identified from morphological features in the microbial colonies (Fig. 1D). As a summary of our observations of the gypsum rocks, a schematic is presented (Fig. 1E) of the microorganisms colonizing rocks under xeric stresses (1).

To further investigate the microbe–substrate interface, we applied a combination of elemental and structural analyses to

the colonized gypsum rocks. Specifically, elemental information from the rock was obtained using energy-dispersive X-ray spectroscopy (EDS) and mapping. In addition to the main elements in gypsum (S, Ca, O, and C), Si, Al, Mg, Na, and Fe were also found (Fig. 2A–C), most likely from sepiolite, a clay mineral previously found in gypsum from the Atacama Desert (SI Appendix, Fig. S4) (6, 8). Structural information, specifically, the phases existing in the gypsum rocks, were identified using X-ray diffraction (XRD) in areas with and without the microorganisms (Fig. 2D). Interestingly, anhydrite was observed in areas populated with microorganisms, while substrate areas without microorganisms consisted only of gypsum. Fourier transform infrared spectroscopy (FTIR) maps were acquired in the areas with microorganisms to further verify the existence of anhydrite phase (21, 26). The resulting spectrum shows a reduction in the intensity of peaks representative of water of crystallization (Fig. 2E, highlighted in orange), suggesting a transformation to anhydrite in that region. FTIR mapping (Fig. 2F and G) further validated the existence of an anhydrite phase around the gypsum phase. These results indicate that the microorganisms are likely responsible for the transformation of gypsum to the anhydrite phase. In previous studies, it has been shown that gypsum can transform to anhydrite by losing its water of crystallization when annealing at 440 K (27). Thus, it is plausible that microorganisms can also drive this transformation by extracting the water they require for survival. To test this hypothesis, culture experiments were performed in a laboratory under controlled conditions.

### Gypsum as a Source of Water for Microorganisms

Gypsum rock samples collected in the Atacama Desert were used as substrate in culture experiments with a cyanobacterium strain, previously isolated from similar samples (Fig. 3A). Gypsum coupons (0.5 × 0.8 × 0.5 mm average size pieces of gypsum rocks) were subjected to two different culture conditions: 1) cyanobacteria in “dry conditions” (defined as only adding the inoculum to the substrate and leaving it to dry during the incubation period) and 2) cyanobacteria in “wet conditions” (defined as adding culture medium to the substrate during the incubation period, in addition to the inoculum). At a 30-d incubation period, cells on, and within, the gypsum coupons had a bright green color, indicating the presence of photosynthetic pigments (Fig. 3B). The presence and distribution of the cyanobacteria within the substrate were further validated by the coexistence of carbon and nitrogen, by EDS mapping (Fig. 3C) and SEM imaging (Fig. 3D). All of the gypsum coupons

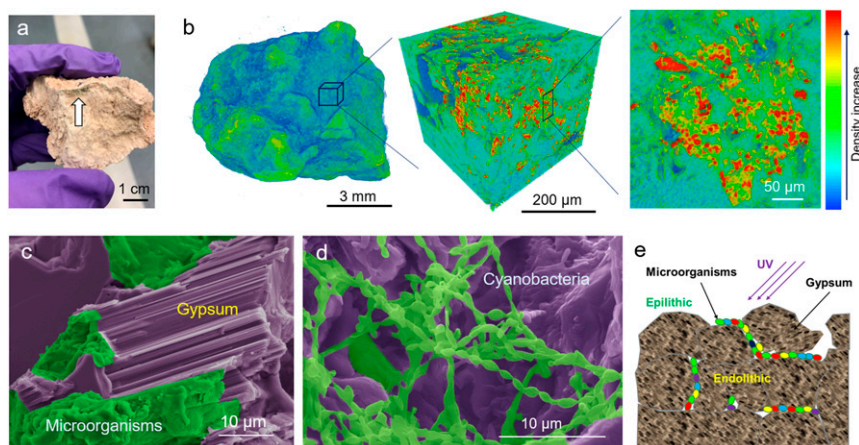


**Fig. 1.** Microorganisms live within gypsum rocks from the Atacama Desert. (A) Photo of gypsum rock samples. The green color indicated with a white arrow shows the area colonized by microorganisms. (B) μ-CT images of gypsum rocks, highlighting the microorganisms living within. The yellow and red colors represent microorganism colonies inside the rock. (C and D) SEM images of gypsum. The extracellular matrix surrounding cyanobacteria cells in gypsum samples is indicated in green in D. (E) Diagram of the microbe colonization and their location in the gypsum rock. UV, ultraviolet.

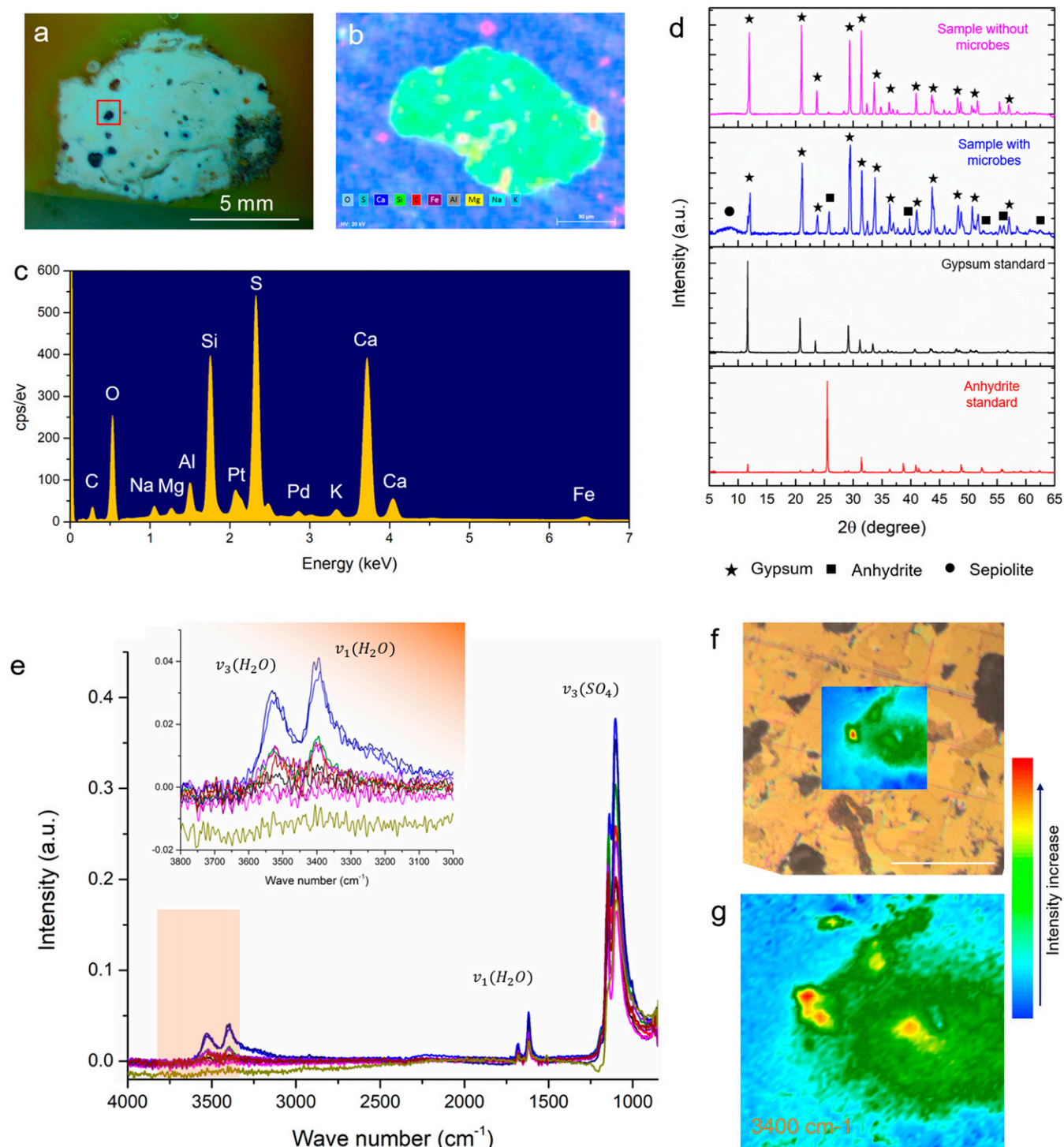


**Fig. 2.** Structure and chemistry of gypsum rocks sample from the Atacama Desert. (A) Optical microscopy of a thin cross-section of the gypsum sample with black impurities within the rocky matrix. (B) Energy-dispersive X-ray (EDX) mapping on gypsum rock samples. The mapping area is indicated by red box in A. The white area is gypsum, while the black area shows Si, Al, Mg, O, and Fe. (C) Average spectrum (counts per second [cps] versus energy) of the EDX mapping in B. (D) XRD of gypsum samples in the areas with and without microbes. Anhydrite phase is observed in areas with microbes. (E) FTIR mapping and spectra of area with microbes in gypsum rocks. The highlighted area, also shown in the *Inset*, from 3,000  $\text{cm}^{-1}$  to 3,800  $\text{cm}^{-1}$  indicates the presence of water of crystallization peaks in the gypsum crystals. (F) Optical microscopy image shows the mapping area. (Scale bar, 100  $\mu\text{m}$ .) (G) FTIR map of peak intensity at 3,400  $\text{cm}^{-1}$ , indicating the water of crystallization in the gypsum crystals. Blue area represents the anhydrite phase, while green and yellow color indicate the existence of gypsum.

harbored cyanobacteria cells; however, due to the difference in the culture conditions, the final composition of the gypsum substrate was different. XRD reveals that anhydrite was present in gypsum coupons cultured in “dry conditions,” but was not

found in gypsum without microorganisms (negative control) or those cultured under hydrated conditions (i.e., in a liquid medium; Fig. 3E). This suggests that the “dry conditions” promoted the extraction of water by cyanobacteria from the gypsum rock,



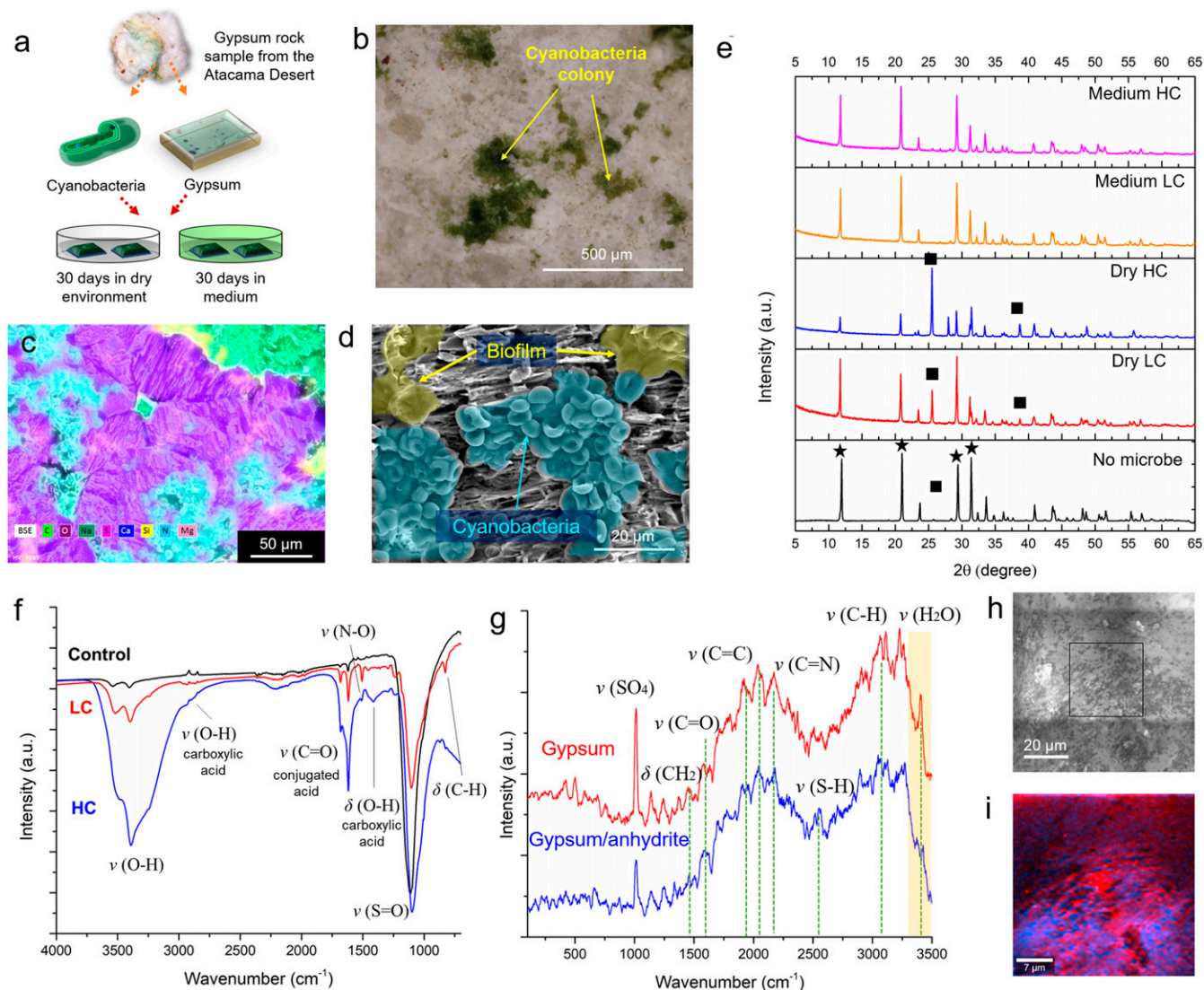


**Fig. 3.** Cyanobacteria culture on gypsum samples. (A) Schematic of cyanobacteria cultured in dry and liquid media. (B) Optical microscopy image of gypsum samples showing colony of cyanobacteria (green color) on the gypsum after culture experiments. (C) EDS mapping of cyanobacteria cultured on the gypsum. (D) SEM images of gypsum sample after culture, showing a porous structure and attachment of cyanobacteria (green color) on the surface. Biofilm is found surrounding the cyanobacteria. (E) XRD of gypsum rock control (black curve; i.e., not exposed to microbes), samples cultured in low concentration (LC) and high concentration (HC) of cyanobacteria in both dry and liquid medium environments. Diffraction peaks labeled with black squares represent the anhydrite phase, while those labeled with stars are from gypsum. (F) FTIR of samples in the control group and the cyanobacteria cultures at low and high concentrations. Specific absorption bands, representing organic acids, are found on the surfaces of the gypsum samples with cyanobacteria cultures. (G) Raman spectroscopy of gypsum samples cultured with a high concentration of cyanobacteria. Both gypsum and anhydrite are detected on the sample surface. Red and blue spectra represent two different areas indicated in *I*. Absorption from water in gypsum is marked with a yellow band. (H and I) Mapping of gypsum and anhydrite phases from Raman spectroscopy. (H) Optical micrograph shows the mapping area (black box) used in *I*. (I) Gypsum (red) and anhydrite (blue) phase map.

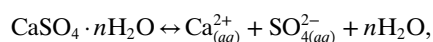
which leads to its transformation to anhydrite. These results corroborate our observations of gypsum rocks collected from the Atacama Desert. More importantly, we found that the XRD peak intensity of the anhydrite phase was greater in coupons cultured with a higher number of cyanobacteria cells, further validating our hypothesis on the role of microorganisms in the phase transformations observed in gypsum.

SEM analysis of the cultured gypsum also showed the presence of an extracellular material forming a biofilm-like matrix that covered the cyanobacteria (Fig. 3D and *SI Appendix, Fig. S5*) (28). FTIR analysis of gypsum coupons cultured with high concentrations of cyanobacteria showed significantly more intense absorption bands for C=O and O-H, indicating the existence of higher concentrations of organic material. Here, it is likely that this organic is rich in carboxylic acid moieties (Fig. 3F)

(26, 29, 30). The presence of organic acids in the biofilm surrounding the cyanobacteria cells was also confirmed by Raman spectroscopy (Fig. 3G) (31–33). In addition, subsequent Raman maps highlight the phase transformation from gypsum to anhydrite (Fig. 3H, pure gypsum and Fig. 3I, a mixture of gypsum and anhydrite). Based on these results, it is likely that the organic acids in the biofilm reacted and etched the gypsum rock, releasing water in its lattice to the cyanobacteria. As the bacteria grow, they produce more organic acid and thus extract additional water that induces further transformation of gypsum. Similarly, bacterial biofilms on tooth surfaces have also been verified to contain acids (i.e., lactic acid) that could lead to the dissolution of calcium phosphate and the decay of tooth enamel (34, 35).

## Mechanisms of Gypsum–Anhydrite Phase Transformation

In order to better understand the transformation of gypsum to anhydrite by these microorganisms, SEM and transmission electron microscopy (TEM) micrographs of both gypsum and anhydrite crystals at different stages of transformation were acquired. Based on our observations, we describe the gypsum–anhydrite phase transformation in four sequential stages (Fig. 4). Initially, microorganisms attach and form a biofilm onto {011} planes of gypsum particles (Fig. 4A and *SI Appendix*, Fig. S1). Prior to any interaction with microbes, the gypsum particles are single crystalline (as observed by TEM in Fig. 4B). The biofilm that is coating the gypsum (Fig. 4A and C and *SI Appendix*, Fig. S4) contains organic acids (19) that induce mineral dissolution, enabling the extraction of water that can be acquired by the microorganisms. Observation of the surface of the gypsum samples reveals a porous structure decorated with biofilm bridges, which is suggestive of the driving force behind mineral dissolution (Fig. 4C). High-resolution TEM (HRTEM) imaging and selected area electron diffraction (SAED) (Fig. 4D and *H, Inset*, respectively) show anhydrite nanocrystals precipitated randomly near the surface of the dissolving gypsum, which suggests that a gypsum–anhydrite phase transformation is occurring. The phase transformation of gypsum to anhydrite has two processes: dissolution of gypsum and precipitation of anhydrite, which can be described as



where  $n$  is the hydration number (19, 36, 37). Thus, the phase transformation is determined by the solubility of the different phases in this specific environment, and anhydrite has been proved to be a more stable phase and has lower solubility (19, 20). The acidic environment created by the microorganisms as well as the extraction of water can increase and facilitate the phase transformation. As additional anhydrite is formed, these “primary” nanocrystals attach, via short-range alignment, to form hierarchically assembled mesocrystals (Fig. 4E and F). Misalignment of crystal planes from two adjacent nanocrystals formed during an oriented attachment process is observed (*SI Appendix*, Fig. S6). Additional assembly (Fig. 4G and H) of these primary particles yields larger anhydrite particles. A long-range alignment of these nanocrystals along the [002] direction is observed (Fig. 4H), with the interfaces of these aligned primary particles clearly present (see HRTEM micrograph in Fig. 4H, *Inset*).

A schematic of the cyanobacteria-induced gypsum–anhydrite phase transformation mechanism is illustrated in Fig. 4I. Microorganisms attached preferentially to the {011} planes in the original gypsum samples found in the Atacama Desert (Fig. 1C and *SI Appendix*, Fig. S5). This is also observed in the controlled cyanobacteria culture experiments (Fig. 4A). Examination of the crystal structure of gypsum (*SI Appendix*, Fig. S7) shows that the water within the mineral was exposed at the {011} planes, but is shielded by {010} planes (38), which may explain the preferential colonization of these organisms. Upon losing the water of crystallization, the monoclinic gypsum crystals become unstable and transform to orthorhombic anhydrite crystals. The relatively insoluble anhydrite (i.e., under acidic conditions) subsequently precipitates as anhydrite nanocrystals near the surfaces of gypsum (20). As this phase transformation proceeds, the anhydrite nanocrystals appear to align and attach to each other in an ordered manner forming mesocrystals, suggesting that additional growth occurs via a nonclassical pathway (39, 40). This growth mechanism is different from classical crystal growth pathways, which typically occur via monomer-by-monomer addition (40). This oriented attachment of primary particles provides a means to reduce the free energy of the system without Ostwald ripening, yielding larger crystals. This process has also been observed

in gypsum crystal growth mechanisms in synthetic environments (41). The surfaces of the final anhydrite crystals are rough, highlighted by numerous interfaces from the nanocrystals (42, 43).

## Conclusions

Endolithic microorganisms in the Atacama Desert have adapted to their extremely dry environment by using their rocky substrate, such as gypsum, not only to protect themselves from extreme solar irradiance but also as a source of water. Microorganisms, such as cyanobacteria, that inhabit these rocks extract water incorporated within the gypsum lattice (water of crystallization), resulting in the concurrent phase transformation to anhydrite. Organic acids were found in the biofilms surrounding these microorganisms. Subsequent etching occurred on high-energy crystal planes of gypsum, releasing water to the microorganisms. Experiments under controlled conditions with cyanobacteria cultures grown on native gypsum rock samples, also collected in the Atacama Desert, validated the aforementioned observations from the geological environment. Specifically, culturing cyanobacteria on the gypsum rocks in a dry environment resulted in a phase transformation from gypsum to anhydrite, with the extent of phase transformation directly correlated to the number of cells in the culture. No phase transformation was observed under hydrated culture conditions, indicating that water extraction from rock only occurs in environments where water is scarce. Analysis of this phase transformation revealed a specific pathway that involves the dissolution of gypsum phase by organic acids in the microbial biofilms with subsequent precipitation of anhydrite nanocrystals, which then grow by particle attachment. The results from the current study not only provide insight into specific interactions between microorganisms and minerals but may also offer potential strategies for water storage technologies in extreme environments, including extraterrestrial habitats.

## Materials and Methods

**Gypsum Rocks Collection.** Colonized gypsum rocks were collected in the Atacama Desert, Chile (GPS coordinates: 20°43'S, 069°58'W; 944 m above sea level) in March 2018. Samples were stored in sterile Whirlpack bags in a dark and at room temperature (~25 °C) before further processing.

### Materials Characterization.

**SEM and EDS.** Gypsum samples collected from the Atacama Desert were thawed in air for 24 h before SEM/EDS characterization. Gypsum rocks were fractured with a chisel and then sputter coated with Pt/Pd. Fracture surfaces were then imaged using a field emission SEM (MIRA3 GMU; TESCAN) operated at 20 kV. For EDS analysis, gypsum samples were first embedded in epoxy (Epofix Cold-Setting Embedding Resin; Electron Microscopy Sciences), polished flat, and evaluated using an SEM (MIRA3 GMU; TESCAN) operated at 20 kV and a Quantax 400 EDS system equipped with dual xFlash 6 SSD detectors (Bruker).

**Powder XRD.** Areas with and without green colonies in the gypsum rocks were isolated and ground into fine powders. An X-ray diffractometer (Empyrean; PANalytical) with Cu-K $\alpha$  radiation with a generator voltage of 45 kV and tube current of 40 mA was used. The scan range (2 $\theta$ ) was from 10° to 70°.

**FTIR.** Gypsum rock samples were embedded in epoxy. An ultramicrotome (RMC MT-X; Boeckeler Instruments) was used to provide smooth sample surfaces for FTIR mapping. A 70  $\times$  70  $\mu\text{m}$  map was created using an FTIR spectrometer (Cary 600 series; Agilent Technologies) with an attenuated total reflection germanium crystal.

**Raman spectroscopy.** Gypsum coupons, after culturing with a high-concentration cyanobacteria, were examined by Raman spectroscopy performed with a WITec confocal Raman microscope fitted with a thermoelectrically cooled charged-coupled device camera and a broadband UHTS300 spectrometer in the visible to near-infrared range, coupled with a MIRA3-TESCAN SEM. The spectra were collected using a Zeiss 100 $\times$  objective in the SEM chamber under vacuum with a 532-nm laser. A 40  $\times$  40  $\mu\text{m}$  map was obtained on the surface of the gypsum coupon.

**TEM.** Embedded gypsum samples sectioned with an ultramicrotome (RMC MT-X; Boeckeler Instruments) to get electron transparent sections (~70 nm). A Field Electron and Ion Company (FEI) Tecnai12 (operated at 120 KV) and an



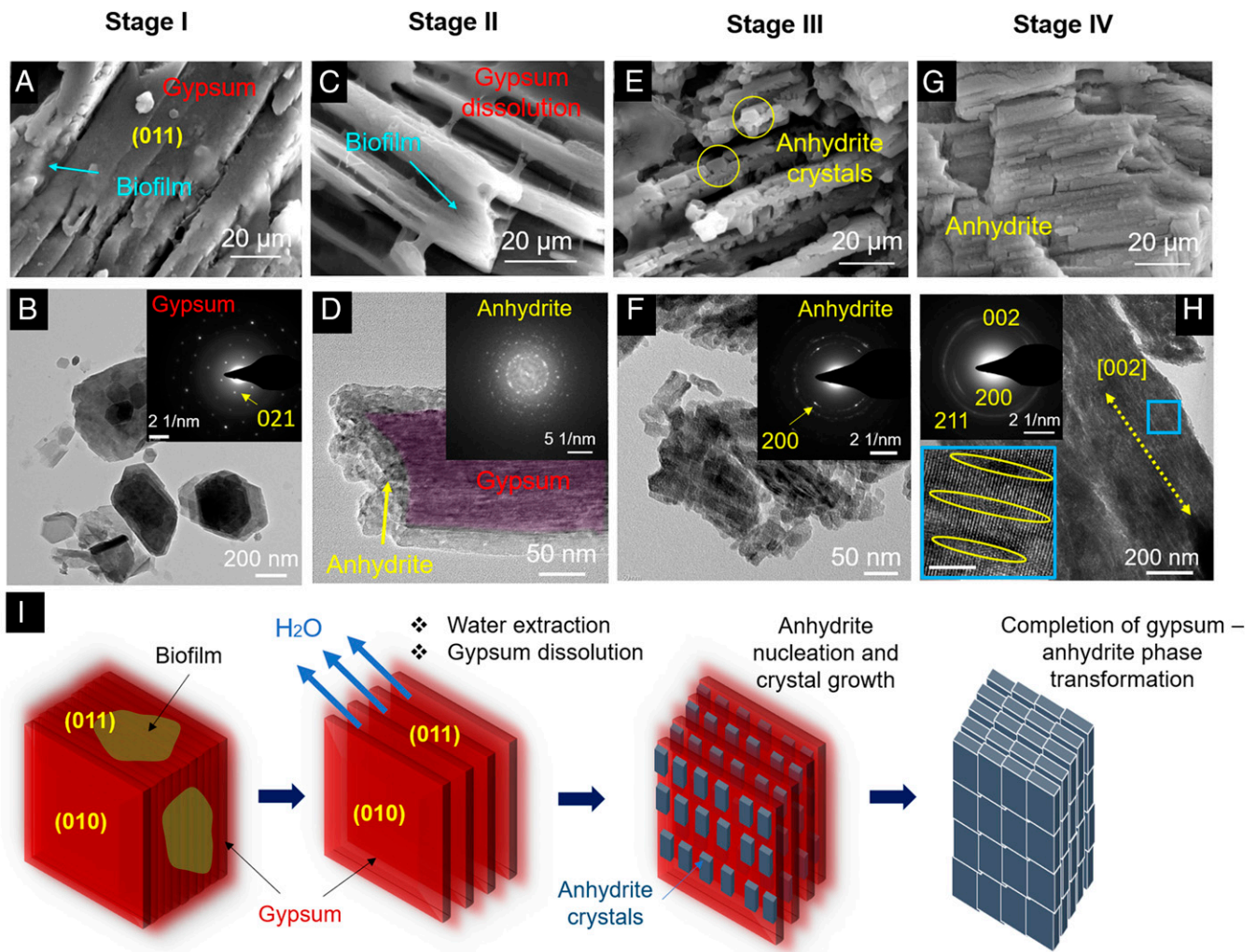


**Fig. 4.** Mechanisms of gypsum–anhydrite phase transformation. The process is described in four stages. Stage I: microorganisms attach on the gypsum crystals and form a biofilm. (A and B) SEM and TEM images highlight the gypsum crystals. Confirmation of single crystalline gypsum provided through TEM and SAED (*Inset*) is shown in B. Stage II: (C and D) gypsum dissolution and water extraction with subsequent anhydrite nanocrystal precipitation. (C) A porous structure is observed at the periphery of the gypsum particles, indicating their dissolution. (D) Anhydrite nucleation on the surface of gypsum crystals. SAED analysis (*Inset*) provides evidence for the random distribution of the anhydrite nanocrystals. Stage III: (E and F) Anhydrite crystal growth. (E) SEM image shows large, faceted, anhydrite particles on the surface of gypsum. (F) Bright-field TEM demonstrates the short-range alignment of anhydrite nanocrystals, suggesting particle attachment. The SAED pattern (*Inset*) indicates alignment of the nanocrystals during the attachment process. Stage IV: (G and H) Completion of the gypsum–anhydrite phase transformation. (G) SEM image of anhydrite particles, highlighting surface faceting. (H) Bright-field TEM image and SAED indicate a preferential alignment along the [002] direction. The blue box (*Inset*) shows the interfaces between nanocrystals observed through HRTEM, indicated with yellow circles. (Scale bar, 5 nm.) (I) Summary and schematic of microorganism induced gypsum–anhydrite phase transformation. Microorganisms attach and form biofilms on the {011} planes of gypsum crystals; gypsum dissolves, and water extraction occurs. Based on the crystal structure of gypsum, the water of crystallization layer is exposed to the {011} planes, but not to the {010} planes. As the single crystalline gypsum dissolves and loses water of crystallization, it transforms via precipitation of nanocrystalline anhydrite. These anhydrite nanocrystals precipitate on the surfaces of gypsum crystals. Short-range alignment of the anhydrite nanocrystals is observed. Large micrometer-sized anhydrite crystals are formed via particle attachment and alignment.

FEI Titan Themis 300 (operated at 300 kV; Thermo Fisher Scientific) were used to obtain bright-field TEM and HRTEM images, respectively.

**Cyanobacteria Isolation, Culture, and Analysis.** A cyanobacterium isolate was obtained by incubating ground colonized gypsum collected in the Atacama Desert (6) in BG11 liquid medium (44, 45) for 5 wk at 25 °C, under 24  $\mu\text{mol photons}\cdot\text{m}^{-2}\cdot\text{s}^{-1}$  of white light. Colonies were isolated from 1% agar (wt/vol) BG11 medium, and the isolate G-MTQ-3P2 was identified as *Chroococcidiopsis* sp. using 16S ribosomal RNA gene sequencing.

Gypsum coupons (0.5 mm  $\times$  0.8 mm  $\times$  ~0.5 mm thick) were prepared using a diamond saw. For culture experiments, coupons were sterilized by autoclaving (20 min at 121 °C) and placed in 96 well plates. One hundred microliters of cyanobacteria culture (isolate G-MTQ-3P2), grown in BG11 medium, were used to inoculate each gypsum coupon at two cell densities,

$10^5$  cells/mL or  $10^8$  cells/mL. Controls were inoculated in a sterile BG11 medium; 96-well plates were incubated at 25 °C under 24  $\mu\text{mol photons}\cdot\text{m}^{-2}\cdot\text{s}^{-1}$  of white light or in the dark for 30 d, either under “wet” or “dry” conditions. Under “wet conditions,” BG11 medium was added periodically to keep a thin liquid layer on top of each coupon. Under “dry conditions,” no additional medium was added during the incubation period. One sample from each condition was ground into a fine powder for XRD (Empyrean; PANalytical). SEM, TEM, and FTIR characterization was performed on the remaining samples, based on the aforementioned methods.

**Data Availability.** All data that support the findings of this study are self-inclusive.

**ACKNOWLEDGMENTS.** We thank Dr. Krassimir Bozhilov at University of California, Riverside for help with TEM analysis. This work was supported by

funding from NASA (Grant NNX15AP18G) to J.D. and the Army Research Office (ARO) (Grant W911NF-18-1-0253) to D.K. and J.D. Also, D.K.

acknowledges funding from ARO (Grants W911NF-16-1-0208 and W911NF-17-1-0152).

1. P. H. Lebre, P. De Maayer, D. A. Cowan, Xerotolerant bacteria: Surviving through a dry spell. *Nat. Rev. Microbiol.* **15**, 285–296 (2017).
2. W. Huang *et al.*, Multiscale toughening mechanisms in biological materials and bio-inspired designs. *Adv. Mater.* **31**, e1901561 (2019).
3. S. B. Pointing, J. Belnap, Microbial colonization and controls in dryland systems. *Nat. Rev. Microbiol.* **10**, 551–562 (2012).
4. J. J. Walker, N. R. Pace, Endolithic microbial ecosystems. *Annu. Rev. Microbiol.* **61**, 331–347 (2007).
5. E. B. Qu *et al.*, Trophic selective pressures organize the composition of endolithic microbial communities from global deserts. *Front. Microbiol.* **10**, 2952 (2020).
6. V. Meslier *et al.*, Fundamental drivers for endolithic microbial community assemblies in the hyperarid Atacama Desert. *Environ. Microbiol.* **20**, 1765–1781 (2018).
7. J. Wierzchos *et al.*, Microbial colonization of Ca-sulfate crusts in the hyperarid core of the Atacama Desert: Implications for the search for life on Mars. *Geobiology* **9**, 44–60 (2011).
8. J. Wierzchos *et al.*, Adaptation strategies of endolithic chlorophototrophs to survive the hyperarid and extreme solar radiation environment of the Atacama Desert. *Front. Microbiol.* **6**, 934 (2015).
9. C. P. McKay *et al.*, Temperature and moisture conditions for life in the extreme arid region of the Atacama desert: Four years of observations including the El Niño of 1997–1998. *Astrobiology* **3**, 393–406 (2003).
10. J. Wierzchos *et al.*, Ignimbrite as a substrate for endolithic life in the hyper-arid Atacama Desert: Implications for the search for life on Mars. *Icarus* **224**, 334–346 (2013).
11. N. Middleton, D. Thomas, *World Atlas of Desertification*, (Edward Arnold, London, United Kingdom, 1992).
12. A. Stevenson *et al.*, *Aspergillus penicillioides* differentiation and cell division at 0.585 water activity. *Environ. Microbiol.* **19**, 687–697 (2017).
13. K. E. Fishbaugh, F. Poulet, V. Chevrier, Y. Langevin, J. P. Bibring, On the origin of gypsum in the Mars north polar region. *J. Geophys. Res. Planets* **112**, E07002 (2007).
14. D. T. Vaniman *et al.*, Magnesium sulphate salts and the history of water on Mars. *Nature* **431**, 663–665 (2004).
15. A. E. Van Driessche, T. M. Stawski, L. G. Benning, M. Kellermeier, Eds., *New Perspectives on Mineral Nucleation and Growth* (Springer, 2017), pp. 227–256.
16. A. Escudero, S. Palacio, F. T. Maestre, A. L. Luzuriaga, Plant life on gypsum: A review of its multiple facets. *Biol. Rev. Camb. Philos. Soc.* **90**, 1–18 (2015).
17. S. Palacio, J. Azorin, G. Montserrat-Martí, J. P. Ferrio, The crystallization water of gypsum rocks is a relevant water source for plants. *Nat. Commun.* **5**, 4660 (2014).
18. C. Zanbak, R. C. Arthur, Geochemical and engineering aspects of anhydrite/gypsum phase transitions. *Environ. Eng. Geosci.* **xxiii**, 419–433 (1986).
19. G. Azimi, V. Papangelakis, J. Dutrizac, Modelling of calcium sulphate solubility in concentrated multi-component sulphate solutions. *Fluid Phase Equilib.* **260**, 300–315 (2007).
20. G. Azimi, V. G. Papangelakis, Mechanism and kinetics of gypsum–anhydrite transformation in aqueous electrolyte solutions. *Hydrometallurgy* **108**, 122–129 (2011).
21. J. L. Bishop *et al.*, Spectral properties of Ca-sulfates: Gypsum, bassanite, and anhydrite. *Am. Mineral.* **99**, 2105–2115 (2014).
22. P. Ballirano, E. Melis, Thermal behaviour and kinetics of dehydration of gypsum in air from in situ real-time laboratory parallel-beam X-ray powder diffraction. *Phys. Chem. Miner.* **36**, 391–402 (2009).
23. E. Finot, E. Lesniewska, J.-C. Mutin, J.-P. Goudonnet, Investigations of surface forces between gypsum microcrystals in air using atomic force microscopy. *Langmuir* **16**, 4237–4244 (2000).
24. P. Feng, A. S. Brand, L. Chen, J. W. Bullard, *In situ* nanoscale observations of gypsum dissolution by digital holographic microscopy. *Chem. Geol.* **460**, 25–36 (2017).
25. A. J. Pinto *et al.*, AFM study of the epitaxial growth of brushite (CaHPO<sub>4</sub>·2H<sub>2</sub>O) on gypsum cleavage surfaces. *Am. Mineral.* **95**, 1747–1757 (2010).
26. Y. Liu, A. Wang, J. Freeman, “Raman, MIR, and NIR spectroscopic study of calcium sulfates: Gypsum, bassanite, and anhydrite” in *40th Lunar and Planetary Science Conference*, (Lunar and Planetary Institute, 2009).
27. L. Sarma, P. Prasad, N. Ravikumar, Raman spectroscopic study of phase transitions in natural gypsum. *J. Raman Spectrosc.* **29**, 851–856 (1998).
28. H.-C. Flemming, J. Wingender, The biofilm matrix. *Nat. Rev. Microbiol.* **8**, 623–633 (2010).
29. D. Das, T. N. Veziroğlu, Hydrogen production by biological processes: A survey of literature. *Int. J. Hydrogen Energy* **26**, 13–28 (2001).
30. J. Schmitt, H.-C. Flemming, FTIR-spectroscopy in microbial and material analysis. *Int. Biodeterior. Biodegradation* **41**, 1–11 (1998).
31. B. Berenblut, P. Dawson, G. Wilkinson, The Raman spectrum of gypsum. *Spectrochim. Acta A* **27**, 1849–1863 (1971).
32. H. G. Edwards, S. E. J. Villar, J. Parnell, C. S. Cockell, P. Lee, Raman spectroscopic analysis of cyanobacterial gypsum halotrophs and relevance for sulfate deposits on Mars. *Analyst* **130**, 917–923 (2005).
33. J. Jehlička, H. Edwards, Raman spectroscopy as a tool for the non-destructive identification of organic minerals in the geological record. *Org. Geochem.* **39**, 371–386 (2008).
34. M. Hannig, C. Hannig, Nanomaterials in preventive dentistry. *Nat. Nanotechnol.* **5**, 565–569 (2010).
35. S. E. Cross *et al.*, Evaluation of bacteria-induced enamel demineralization using optical profilometry. *Dent. Mater.* **25**, 1517–1526 (2009).
36. B. Messnaoui, T. Bounahmidi, On the modeling of calcium sulfate solubility in aqueous solutions. *Fluid Phase Equilib.* **244**, 117–127 (2006).
37. Y. Tang, J. Gao, C. Liu, X. Chen, Y. Zhao, Dehydration pathways of gypsum and the rehydration mechanism of soluble anhydrite  $\gamma$ -CaSO<sub>4</sub>. *ACS Omega* **4**, 7636–7642 (2019).
38. D. Aquilano, F. Otálora, L. Pastero, J. M. García-Ruiz, Three study cases of growth morphology in minerals: Halite, calcite and gypsum. *Prog. Cryst. Growth Charact. Mater.* **62**, 227–251 (2016).
39. J. J. De Yoreo *et al.*, CRYSTAL GROWTH. Crystallization by particle attachment in synthetic, biogenic, and geologic environments. *Science* **349**, aaa6760 (2015).
40. M. Niederberger, H. Cölfen, Oriented attachment and mesocrystals: Non-classical crystallization mechanisms based on nanoparticle assembly. *Phys. Chem. Chem. Phys.* **8**, 3271–3287 (2006).
41. T. M. Stawski *et al.*, Formation of calcium sulfate through the aggregation of sub-3 nanometre primary species. *Nat. Commun.* **7**, 11177 (2016).
42. T. Wang, H. Cölfen, M. Antonietti, Nonclassical crystallization: Mesocrystals and morphology change of CaCO<sub>3</sub> crystals in the presence of a polyelectrolyte additive. *J. Am. Chem. Soc.* **127**, 3246–3247 (2005).
43. H. Cölfen, M. Antonietti, Mesocrystals: Inorganic superstructures made by highly parallel crystallization and controlled alignment. *Angew. Chem. Int. Ed. Engl.* **44**, 5576–5591 (2005).
44. R. Rippka, J. Deruelles, J. B. Waterbury, M. Herdman, R. Y. Stanier, Generic assignments, strain histories and properties of pure cultures of cyanobacteria. *Microbiology* **111**, 1–61 (1979).
45. W. V. Sigler, R. Bachofen, J. Zeyer, Molecular characterization of endolithic cyanobacteria inhabiting exposed dolomite in central Switzerland. *Environ. Microbiol.* **5**, 618–627 (2003).